A: XXXIX-0000

AN OVERVIEW OF LOCAL AND DISTORTIONAL BUCKLING IN COLD-FORMED LIPPED CHANNEL SECTIONS IN FLEXURE

Lucas Fadini Favarato (1) (A); Daniel Carvalho de Moura Candido (2); André Vasconcelos Soares Gomes (3); Johann Andrade Ferrareto (4); Juliana da Cruz Vianna (5); Adenilcia Fernanda Groberio Calenzani (6)

(1) Civil Engineer, M.Sc., ArcelorMittal Tubarão. Vitória, Brazil.
(2) Civil Engineer, M.Sc., Federal University of Espírito Santo. Vitória, Brazil.
(3) Civil Engineer, M.Sc., ArcelorMittal Tubarão. Vitória, Brazil.
(4) Civil Engineer, D.Sc., ArcelorMittal Construction. France.
(5) Professor, D.Sc., Federal University of Espírito Santo. Vitória, Brazil.
(6) Professor, D.Sc., Federal University of Espírito Santo. Vitória, Brazil.
Contact: lucasffavarato@gmail.com; (A) Presenter.

Thematic area: Theoretical models.

Abstract

The design of cold-formed steel elements in flexure can be easily performed by the Direct Strength Method – a simplified alternative based on experimental data, in which the critical buckling bending moments are needed to assess the ultimate resistance of steel elements. Whereas numerous theoretical models are found in the literature to appraise local and distortional buckling loads, they're usually based on simplifications and don't provide their exact values so that different formulations conduct to different results. In this sense, through analyses based on the Finite Element and the Finite Strip Methods, this work seeks to numerically obtain local and distortional buckling loads of a cold-formed U stiffened section bent about both principal axes and compare the results with those provided by the theoretical models. While numerical results have shown good agreement between them, with deviations less than 5% on mean, the analytical ones seemed to be conservative but not accurate when compared to the firsts, with deviations varying from 7% up-to 60%.

Keywords: Cold-formed design; Direct strength method; Local and distortional buckling.

1. INTRODUCTION

The modernization in structural engineering and the new market demands for most efficient solutions in the last years highlighted the use of light steel structures in civil construction, which is owed to assemblage facilities and quality in the final product. Besides, the major advantage achieved is related to fabrication process, in which thin plates, with apparently no structural resistance, are stiffened where buckling can occur. Thus, the cold-formed steel (CFS) profiles are obtained from thin plates folding, whit thicknesses varying between 0.4 and 8.0 mm according to the NBR 14762 (ABNT, 2010), granting a good variety of shapes and an appropriate mass/resistance relation as well (JAVARONI, 2015).

These structures are suitable for small and medium structures such as warehouses, roof structures, mezzanines and houses (SILVA, PIERIN, SILVA, 2014). In addition, new solutions for composite slabs with cold-formed incorporated profiles have arrived to the market, in which stiffened U sections usually act as formwork before concrete curing and can act as steel reinforcements after concrete curing.

The design of cold-formed profiles, in this context, can be performed by three different methods, in accordance with different Design Codes, such as NBR 14762 (ABNT, 2010), AZ/NZS 4006 (AZ/NZS, 2005) and AISI S100 (AISI, 2016). The first one, the Effective Width Method, analyses the effectiveness of each part of the gross section subjected to the correspondent flexural stress (flanges, webs and stiffeners) in order to define the effective section and its effective properties (YU, LABOUBE, 2010). This approach, on the other hand, leads to long and iterative calculations and does not provide a simple strategy to analyze distortional buckling. The second one, the Effective Section Method, was proposed by Batista (2010) and, based on experiments, considers an elastic buckling critical bending moment to calculate the cross section effective properties. The third, last and most simple one, the Direct Strength Method (DSM), suggests the use of experimental resistance equations to evaluate the ultimate resistance of elements in flexure, directly based on the gross cross section properties. Once this procedure considers three limit-states related to global, distortional and local buckling, these critical loads must be obtained to determine the reduced slenderness of steel elements and evaluate the ultimate resistance.

The Brazilian National Code NBR 14762 (ABNT, 2010) states that, when dealing with global buckling of cold-formed members in bending, the exact value of lateral-torsional critical moment can be straightly evaluated from analytical formulations. On the other hand, whereas numerous models are found in the literature to assess local and distortional critical moments, each model is based on different simplifications and assumptions so that values obtained with different formulations lead to different results. The NBR 14762 (ABNT, 2010), for example, recommends the use of Elastic Stability Theory in the treatment of local and distortional buckling modes.

Nonetheless, buckling analysis in cold-formed members is a quite deep and relevant field of research, since it directly impacts the design of steel elements under compression and bending in special when the Direct Strength Method is applied. In this sense, many researches worldwide have investigated the occurrence of local, distortional, global or coupled modes of buckling in CFS profiles under different conditions, such as Kown and Hancock (1992), Schafer and Pekoz (1998), Yu and Schafer (2003, 2006), Kankanamge and Mahendran (2012), Basaglia and Camotion (2013) and Glauz (2017). Pala (2006), who wrote the most noticed paper, proposed a new formulation to calculate the critical distortional stress using neural networks, being the results compared to different methods.

In this sense, a comparative analysis based on numerical approaches is implemented in this paper, what helps dealing with local and distortional buckling in cold-formed beams. The Finite Element Method (FEM) and the Finite Strip Method (FSM) were selected and used to numerically obtain the critical loads for the issued buckling modes. Then, the accuracy of each selected theoretical model – NBR 14762 (ABNT, 2010), AISI S100 (AISI, 2016), NBR 14762 (ABNT, 2001), Sharp *apud* Hancock (1997), Ellifritt, Glover and Hren (1998) and Douty (1962) – could be determined.

2. REVIEW OF THE LITERATURE

In this topic, theoretical models for the assessment of critical buckling moments are presented, the basis for the comparative analysis performed afterwards.

1. Local buckling

When a CFS channel section, stiffened or not, is subjected to the action of a bending moment, each plate that composes webs, flanges or stiffeners behaves as a single element in bending and, thus, moves out of the cross-sectional plane. Although, the junction remains fixed in its original position. This phenomenon, understood as a consequence of plate flexure, is known as local buckling (CARVALHO, GRIGOLETTI, BARBOSA, 2014). If the section is bent about the major inertia axis, compressing the flange or the flange and stiffener set, the out-of-plane observed displacements are a consequence of plates in bending. Besides, plates with free edges that compose the stiffeners only suffer rigid body rotation, according to Figure 1a (MELO, 2017). On the other hand, a rigid body rotation can be observed in the stiffeners and bending in the flanges when flexure happens about the minor axis, compressing the flange and stiffener set as well (Figure 1b).

(a) (b)

Figure 1. Cross section under local buckling: (a) bending about the major axis; (b) bending about the minor axis.
Source: CUFSM 5.01 (SCHAFER, 2016).

Two theoretical models for the determination of critical bending moments related to local buckling (M_l) were selected, for both cases presented in Figure 1. Notice that W_c indicates the elastic resistance modulus of the gross cross section about the bending axis.

For flexure about the major axis of inertia:

a) National Brazilian Code NBR 14762 (ABNT, 2010), according to Eq. (1), where k_l is the local buckling coefficient for the whole section, taken from Table 12 of the NBR 14762

(ABNT, 2010); b_w is the profile's height; t is the plate thickness; E is the Young's Modulus; and ν is the Poisson's ratio, taken as 0.3.

$$M_l = k_l \frac{\pi^2 E}{12(1-\nu^2)\left(\frac{b_w}{t}\right)^2} W_c \qquad 1$$

For flexure about the minor axis of inertia:

a) North-American Code AISI S100 (AISI, 2016), according to Eq. (2), where σ_l is elastic buckling stress in respect of the extremely compressed plate (stiffener, web or flange). This parameter should be calculated in accordance with AISI S100 (AISI, 2016) annexes, whose procedure is too long to be presented in this paper.

$$M_l = \sigma_l W_c \qquad 2$$

2. Distortional buckling

The distortional buckling mode, different from the local one, is only experienced by stiffened sections. The profile dimensions, specially related to flanges and edge stiffeners, are essentials to characterize the distortional buckling. The wider the flange is, higher are the probabilities to figure this mode as the critical one. Besides, elements made from steel plates with high resistance can also have the distortional mode as critical.

In addition, Chodraui (2003) points out that the distortional buckling in U stiffened sections is defined by the rotation and possible translation of compressed flange and stiffener set. In this case, only the edges not related to stiffener-flange junction remain in their original position, whichever is the bending axis (Figure 2).

(a) (b)

Figure 2. Cross section under distortional buckling: (a) bending about the major axis; (b) bending about the minor axis.
Source: CUFSM 5.01 (SCHAFER, 2016).

In the literature, there are different analytical models to calculate stresses or moments critical of distortional buckling. Five of them were selected and are presented in the sequence. Although, it's important to state that all of these procedures are long and, hence, only a part

summary of them is exhibited here. When only σ_{dist} is provided, then $M_{dist} = \sigma_{dist}\, W_c$, where σ_{dist} is the distortional buckling critical stress and M_{dist} is the distortional buckling critical moment.

For flexure about the major axis of inertia:

a) NBR 14762 (ABNT, 2001), according to Eq. (3), where E is the Young's Modulus; A_f is the reduced section's area; and α_1, α_2 and α_3 are parameters that depend on the properties of reduced section. This model assumes the reduced section as the set formed by compressed flange and edge stiffener, replacing the web and web-flange junction by rigid support on the vertical direction and by elastic supports on the other directions.

$$\sigma_{dist} = \frac{E}{2A_f}\left[(\alpha_1 + \alpha_2) - \sqrt{(\alpha_1 + \alpha_2)^2 - 4\alpha_3}\right] \quad (3)$$

b) Sharp *apud* Hancock (1997), according to Eq. (4) and (5), where k_ϕ is the rotational elastic stiffness provided by the web-flange junction. This model, different from the previous one, considers no linear spring supports.

$$\sigma_{dist} = \frac{2\sqrt{EI_{xf}b_f^2 k_\phi} + \frac{EJ_f}{2(1+\nu)}}{I_{xf} + I_{yf} + A_f(\bar{x}^2 + \bar{y}^2)} \quad (4)$$

$$k_\phi = \frac{2Et^3}{5{,}46\left(b_w + \frac{2}{3}b_f\right)} \quad (5)$$

c) Ellifritt, Glover and Hren (1998), according to Eq. (6) and (7), where b_f is the flange width; b_w is the web width; t is the plate thickness; f_y is the steel yield stress, in ksi; and M_y is the bending moment that causes yielding in the section extreme compressed fiber.

$$X = \left(\frac{b_f}{t}\right)^{1,1}\left(\frac{b_w}{D}\right)^{0,4}\frac{f_y}{50} \quad (6)$$

$$\frac{M_{dist}}{M_y} = -\frac{8X^3}{10^9} + \frac{X^2}{10^5} - 0{,}0048X + 1{,}2685 \quad (7)$$

d) AISI S100 (AISI, 2016), according to Eq. (8), where k represent all the rotational stiffness in the web-flange junction: $k_{\phi fe}$ – provided by the flange; $k_{\phi we}$ – provided by the web; k_ϕ – provided by an external element connected to the flange; $\tilde{k}_{\phi fg}$ – required by the flange; and $\tilde{k}_{\phi wg}$ – required by the web; and β a parameter that accounts for the moment gradient, which can be conservatively taken as 1.0.

$$\sigma_{dist} = \beta \frac{k_{\phi fe} + k_{\phi we} + k_{\phi}}{\tilde{k}_{\phi fg} + \tilde{k}_{\phi wg}} \quad (8)$$

For flexure about the minor axis of inertia:

a) Douty (1962), according to Eq. (9), where the conventional distortional buckling stress should be calculated based on the transformed section, only formed by elements in the gross cross section that can experience distortions.

$$\sigma_{dist} = \frac{\pi^2 E}{\lambda_{eq}^2} \frac{d_c}{y_c} \quad (9)$$

3. METHODS

Two numerical experiments were carried out, using different approaches to solve the same problem. At first, the profile Ue100x40x17x1.2 was select to simulate a cold-formed beam with different lengths, bent about both main axes, in order to obtain the critical loads of local and distortional buckling. When bending occurs about the minor axis, the edge stiffeners are intended to be compressed by the action of the moment (sagging bending moment). The experiments are detailed in the sequence.

a) Experiment I: a Finite Element Analysis was conducted using ANSYS® 14.0 (ANSYS, 2011). Several simply supported beams were modeled, being lengths integer multiples of the critical length regarding each buckling mode ($L = nL_{cr}, n = 1,2,3,4,5$), as stated in the first line of each Table 1 to Table 4. In these analyses, the four-node finite element Shell 181 was employed, once it's suitable for linear or non-linear analysis of thin to moderately thin-walled structures, with six degrees of freedom at each node (three displacements and three rotations). The mesh size was adopted in accordance with Candido et al. (2018), who conducted similar buckling experiments in the same cold-formed profile, suggesting that 2 mm x 6 mm is an adequate dimension for the rectangular finite element. In addition, torsional and bending simple supports were provided to constrain the twist and y-direction displacement in the section plane at edges, letting warping free, although. In the web's central node, a single support was provided to constrain longitudinal displacements (z direction), according to Figures 3a and 3b. Then, edge forces were applied assuming an elastic stress distribution (Figures 3c and 3d), resulting into an unitary bending moment – 1 Nm. Finally, the Lanczos Method has been employed for eigenvalue extraction so that 80 critical loads were obtained and processed to identify local and distortional modes

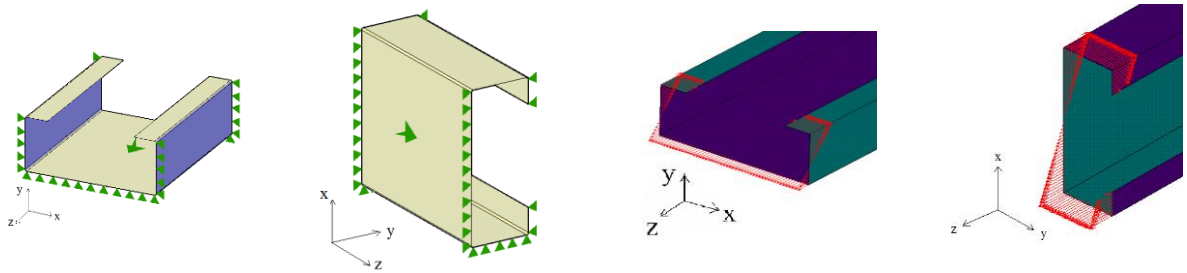

(a) (b) (c) (d)

Figure 3. Information about the finite element model.
Source: Favarato *et al.* (2019).

b) Experiment II: a Finite Strip Analysis was carried out using CUFSM® 5.01 (SCHAFER, 2016), adopting a mesh pattern in the section plane as refined as that used in the previous approach. The cold-formed beams are simply supported and, for the buckling analysis, warping is free.

c) Material's properties: For both analyses, Young's Modulus was assumed as 200 GPa and Poisson's ratio as 0.3, in accordance with Brazilian National Code NBR 14762 (ABNT, 2010). Besides, the steel yield strength was adopted as 340 MPa in the experiment II.

Additionally to the local and distortional buckling loads obtained, the lateral-torsional critical loads were previously determined by Favarato *et al*. (2019) and they were compared to the exact analytical formulation presented in the Brazilian National Code NBR 14762 (ABNT, 2010). The results have shown good agreement as numerical analyzed values deviate only -0.31% when bending happens about the major axis and -4.10% for minor bending, on mean. Thus, the finite element model can be considered as calibrated and appropriate to be employed as reference for the comparative analyses.

4. RESULTS AND DISCUSSIONS

The results obtained are shown in Table 1 to Table 4, where L indicates the span length. It can be observed that the values arisen from theoretical models are conservative in all cases, except for the Sharp *apud* Hancock (1997) model for distortional buckling in beams bent about the minor axis of inertia. The deviations – calculated with basis on the finite element results – observed in the data set stem from simplifications made in the analytical models, derived for bar elements, while numerical experiments have been carried out with shell elements.

When dealing with distortional buckling, the variability and dispersion in the results indicate there's no agreement in the theoretical models in order to provide a single critical bending moment or results close to each other. On the other hand, assuming that the boundary conditions are satisfactory in the finite element model – since they provided excellent results for lateral-torsional buckling as stated by Favarato *et al*. (2019) – and comparing these results with those from the finite strip analyses, both alternatives based on the elastic stability provided confident results, with good agreement between them, differing less than 7% from each other.

For local buckling:

Table 1. Bending about the major axis.

L (cm)	Local buckling bending moment (Nm)			Deviation (%)	
	ANSYS	CUFSM	NBR 14762 (ABNT, 2010)	CUFSM	NBR 14762 (ABNT, 2010)
5.3	5547.67	5320.07	5110.66	-4.10%	-7.88%
3.0	5545.18	5320.07	5110.66	-4.06%	-7.84%
4.0	5544.39	5320.07	5110.66	-4.05%	-7.82%
5.0	5544.07	5320.07	5110.66	-4.04%	-7.82%
6.0	5543.92	5320.07	5110.66	-4.04%	-7.82%
		Average deviation		-4.06%	-7.83%

Table 2. Bending about the minor axis.

L (m)	Local buckling bending moment (Nm)			Deviation (%)	
	ANSYS	CUFSM	AISI S100 (AISI, 2016)	CUFSM	AISI S100 (AISI, 2016)
2.0	2062.00	1970.66	1230.63	-4.43%	-40.32%
3.0	2061.23	1970.66	1230.63	-4.39%	-40.30%
4.0	2060.98	1970.66	1230.63	-4.38%	-40.29%
5.0	2060.85	1970.66	1230.63	-4.38%	-40.29%
6.0	2060.78	1970.66	1230.63	-4.37%	-40.28%
		Average deviation		-4.39%	-40.30%

For distortional buckling:

Table 3. Bending about the major axis.

L (m)	Distortional buckling bending moment (Nm)						Deviation (%)				
	ANSYS	CUFSM	NBR 14762 (ABNT, 2001)	SHARP *apud* HANCOCK (1997)	AISI S100 (AISI, 2016)	ELLIFRITT, GLOVER AND HREN (1998)	CUFSM	NBR 14762 (ABNT, 2001)	SHARP *apud* HANCOCK (1997)	AISI S100 (AISI, 2016)	ELLIFRITT, GLOVER AND HREN (1998)
2.0	5561.59	5182.27	4114.48	5951.90	4306.87	2039.28	-6.82%	-26.02%	7.02%	-22.56%	-63.33%
3.0	5561.55	5182.27	4114.48	5951.90	4306.87	2039.28	-6.82%	-26.02%	7.02%	-22.56%	-63.33%
4.0	5547.84	5182.27	4114.48	5951.90	4306.87	2039.28	-6.59%	-25.84%	7.28%	-22.37%	-63.24%
5.0	5429.37	5182.27	4114.48	5951.90	4306.87	2039.28	-4.55%	-24.22%	9.62%	-20.67%	-62.44%
6.0	5512.44	5182.27	4114.48	5951.90	4306.87	2039.28	-5.99%	-25.36%	7.97%	-21.87%	-63.01%
					Average deviation		-6.15%	-25.49%	7.78%	-22.01%	-63.07%

Table 4. Bending about the minor axis.

L (m)	Distortional buckling bending moment (Nm)			Deviation (%)	
	ANSYS	CUFSM	DOUTY (1962)	CUFSM	DOUTY (1962)
2.0	1709.11	1685.84	1400.01	-1.36%	-18.09%
3.0	1713.24	1685.84	1386.91	-1.60%	-19.05%
4.0	1714.86	1685.84	1382.32	-1.69%	-19.39%
5.0	1708.91	1685.84	1380.20	-1.35%	-19.24%
6.0	1704.52	1685.84	1379.04	-1.10%	-19.10%
		Average deviation		-1.42%	-18.97%

With respect to the design of CFS elements under flexure via DSM, the resistances calculated using the analytical formulations presented herein do not threaten structural safety and stability, since they underestimate buckling loads. Thus, buckling would occur at an early load stage than if correctly calculate with numerical approaches, which gives rise to an uneconomical design philosophy. Setting the coefficient of utilization as the unit, heavier sections would be needed to resist to the same bending moment. In this sense, an unique formulation based on the elastic stability analysis should be determined to standardized critical buckling loads of CFS profiles, especially in minor bending for the distortional mode. This tool is quite important and it's needed by engineers for, at least, preliminary calculations.

5. CONCLUSIONS

In this paper, a set of comparative analyses was performed in order to evaluate the accuracy of some theoretical models found in the literature to determine local and distortional critical loads in cold-formed U stiffened sections. The results suggested that both numerical alternatives produce close results, however different from the analytical ones with deviations more than 40% for some cases.

The calculation of these buckling loads for design solutions can surely make use of analytical models, although leading to sections with more material waste, once they suggest that buckling will occur in a lower stress magnitude. Thus, when results based on the elastic stability analysis are used, buckling loads usually reach more elevated values and allows for optimized design solutions of cold-formed U sections in flexure.

ACKNOWLEDGEMENTS

The authors acknowledge ArcelorMittal Tubarão, Federal University of Espírito Santo, CAPES, CNPq and FAPES for the support during this research.

REFERENCES

AMERICAN IRON AND STEEL INSTITUTE. **AISI S100: North American Specification for the Design of Cold-Formed Steel Structural Members**. 2016.

ANSYS: Engineering Analysis System. Versão 14.0, 2011.

ASSOCIAÇÃO BRASILEIRA DE NORMAS TÉCNICAS. **NBR 14762: Dimensionamento de estruturas de aço constituídas por perfis formados a frio - procedimento.** Rio de Janeiro, 2001.

ASSOCIAÇÃO BRASILEIRA DE NORMAS TÉCNICAS. **NBR 14762: Dimensionamento de estruturas de aço constituídas por perfis formados a frio.** Rio de Janeiro, 2010.

AUSTRALIAN/NEW ZEALAND STANDARD. AZ/NZS 4600**: Cold-formed steel structures.** 253p. 2005.

BASAGLIA, C.; CAMOTIM, D. **Buckling, post-buckling, strength and DSM design of cold-formed steel continuous lipped channel beams.** Journal of Structural Engineering, Vol. 139, No. 5, p. 657–668. ASCE, 2013.

BATISTA, E. M. **Effective section method: A general direct method for the design of steel cold-formed members under local–global buckling interaction.** Thin-Walled Structures, Vol. 48, p. 345–356. Elsevier, 2010.

CÂNDIDO, D. C. M.; STORCH, A. P.; GOMES, A. V. S.; FAVARATO, L. F.; CALENZANI, A. F. G. **Análise numérica de flambagem de perfis de aço formados a frio empregados em lajes nervuradas mistas.** In: XIII SIMMEC – Simpósio de Mecânica Computacional, 2018. Vitória. Anais do XIII Simpósio de Mecânica Computacional.

CARVALHO, P. R. M.; GRIGOLETTI, G.; BARBOSA, G. D. **Curso básico de perfis de aço formados a frio**. 3ª edição, 370p. Porto Alegre: [s. n.], 2014.

CHODRAUI, G. M. B. **Flambagem por distorção da seção transversal em perfis de aço formados a frio submetidos à compressão centrada e à flexão.** 2003. 186p. Dissertação (Mestrado) – Programa de Pós-Graduação em Engenharia de Estruturas, Escola de Engenharia de São Carlos da Universidade de São Paulo. São Carlos.

DOUTY, R. T. **A design approach to the strength of laterally unbraced compression flange.** Engineering Experiment Station, Cornell University, 1962.

ELLIFRITT, D. S.; GLOVER, R. L.; HREN, J. D. A **Simplified Model for Distortional Buckling of Channels and Zees in Flexure.** In: Proceedings of International Specialty Conference on Cold-Formed Steel Structures, University of Missouri-Rolla, Oct. 1998.

FAVARATO, L. F.; CANDIDO, D. C. M.; GOMES, A. V. S.; CALENZANI, A. F. G.; VIANNA, J. C.; FERRARETO, J. A**. Lateral-torsional buckling of cold-formed continuous beams with stiffened U sections bent about the axis of lower inertia.** In: 8º CONGRESSO LATINO-AMERICANO DA

CONSTRUÇÃO METÁLICA, 2019. São Paulo. Proceedings of the 8º Congresso Latino-Americano Da Construção Metálica.

GLAUZ, R. S. **Elastic lateral-torsional buckling of general cold-formed steel beams under uniform moment.** Thin-Walled Structures, Vol. 119, p. 586–592. Elsevier, 2017.

JAVARONI, C. E. **Estruturas de aço: dimensionamento de perfis formados a frio.** 1ª edição. Rio de Janeiro: Elsevier, 2015.

KANKANAMGE, N. D.; MAHENDRAN, M. **Behaviour and design of cold-formed steel beams subjected to lateral-torsional buckling.** Thin-Walled Structures, Vol. 51, p. 25–38. Elsevier, 2012.

KOWN, Y. B.; HANCOCK, G. J. **Tests of cold-formed channels with local and distortional buckling.** Journal of Structural Engineering, Vol. 117, No. 7, p. 1786–1803. ASCE, 1992.

MELO, J. M. S. **Análise da flambagem elástica e da resistência de telhas autoportantes de aço formadas a frio.** 2017. 92p. Dissertação (Mestrado) – UFRJ/COPPE, Programa de Engenharia Civil. Rio de Janeiro.

PALA, M. **A new formulation for distortional buckling stress in cold-formed steel members.** Journal of Constructional Steel Research, Vol. 62, p. 716–722. Elsevier, 2006.

SCHAFER, B. W. **CUFSM 5.01** – Elastic Buckling Analysis of Thin-Walled Members by Finite Strip Analysis. Johns Hopkins University. 2016.

SCHAFER, B. W.; PEKOZ, T. **Direct strength prediction of cold-formed steel members using numerical elastic buckling solutions.** In: Proceedings of 14th International Specialty Conference on Cold-Formed Steel Structures, University of Missouri-Rolla, Oct. 1998.

SHARP (1996) apud. HANCOCK, G. J. **Design for Distortional Buckling of Flexural Members.** Thin-Walled Structures, Vol. 27, No. I, p. 3–12. Elsevier, 1997.

SILVA, E. L., PIERIN, I., SILVA, V. P. S. **Estruturas Compostas por Perfis Formados a Frio:** Dimensionamento pelo Método das Larguras Efetivas e Aplicação conforme ABNT NBR 14762:2010 e ABNT NBR 6355:2012, Instituto do Aço Brasil. Rio de Janeiro, RJ, Brasil, 2014.

YU, C.; SCHAFER, B. W**. Distortional buckling tests on cold-formed steel beams.** Journal of Structural Engineering, Vol. 132, No. 4, p. 515–528. ASCE, 2006.

YU, C.; SCHAFER, B. W. **Local buckling tests on cold-formed steel beams.** Journal of Structural Engineering, Vol. 129, No. 12, p. 1596–1606. ASCE, 2003.

YU, W. W.; LABOUBE, R. A. **Cold-formed steel design.** John Wiley & Sons. 4th edition, 2010.